Summary of Recent Research on Exact Quantum Many-Body Scars

Camilla Polvara

August 29, 2025

Overview

This document summarizes recent research focused on **exact quantum many-body scars** in spin systems, where analytic expressions for the scarred eigenstates are known. These studies circumvent the need to analyze the full Hamiltonian spectrum, instead targeting entanglement properties and reduced density matrices (RDMs) of analytically understood scarred states. All models are assumed to be in 1-dimension and to have periodic boundary conditions (PBC), unless otherwise specified.

1. Dimer State Scar

- **Model:** Spin-1/2 MG-like model featuring an exact dimer scar state.
  This is a one-dimensional spin-$\frac{1}{2}$ model with two- and three-body interactions. The Hamiltonian of the model depends on a parameter $t \in \mathbb{R}$ and is given by

$$H(t) = H_{\mathrm{MG}} + t\, C_{\mathrm{SC}}, \tag{1}$$

  where

$$H_{\mathrm{MG}} = \sum_{j=1}^{L} \left[(\mathbf{S}_j + \mathbf{S}_{j+1} + \mathbf{S}_{j+2})^2 - \frac{3}{4} \right], \tag{2}$$

$$C_{\mathrm{SC}} = \sum_{j=1}^{L} \mathbf{S}_j \cdot (\mathbf{S}_{j+1} \times \mathbf{S}_{j+2}), \tag{3}$$

  and $\mathbf{S}_j = \left(S_j^x, S_j^y, S_j^z\right)$ is the spin-$\frac{1}{2}$ operator acting on site j:

$$S_j^x = \frac{1}{2} \begin{pmatrix} 0 & 1 \\ 1 & 0 \end{pmatrix}_j, \tag{4}$$

$$S_j^y = \frac{1}{2} \begin{pmatrix} 0 & -i \\ i & 0 \end{pmatrix}_j, \tag{5}$$

$$S_j^z = \frac{1}{2} \begin{pmatrix} 1 & 0 \\ 0 & -1 \end{pmatrix}_j. \tag{6}$$

  The first term H_{MG} is the Hamiltonian of the Majumdar-Ghosh model (which has the dimer states as ground states), while the second term C_{SC} is the scalar spin chirality.

There is just one scarred state, which is the ground state of the Majumdar-Ghosh Hamiltonian, and it's given by the singlet state:

$$|\text{dimer}\rangle = \left(2 + \left(-\frac{1}{2}\right)^{\frac{L}{2}-2}\right)^{-\frac{1}{2}} \left(|\Psi_1\rangle + |\Psi_2\rangle\right). \tag{7}$$

where L is the (even) number of sites, and

$$|\Psi_1\rangle = |\text{sing}\rangle_{1,2} \otimes |\text{sing}\rangle_{3,4} \otimes \cdots \otimes |\text{sing}\rangle_{L-1,L}, \tag{8}$$
$$|\Psi_2\rangle = |\text{sing}\rangle_{2,3} \otimes |\text{sing}\rangle_{4,5} \otimes \cdots \otimes |\text{sing}\rangle_{L,1}, \tag{9}$$

are the two dimer states, with

$$|\text{sing}\rangle_{i,j} = \frac{1}{\sqrt{2}} \left(|\uparrow\downarrow\rangle_{i,j} - |\downarrow\uparrow\rangle_{i,j}\right). \tag{10}$$

$|\text{sing}\rangle_{i,j}$ the normalized spin singlet between sites i, j.
The scarred state is annihilated by C_{SC} (as well as by H_{MG}), and thus it is a zero-energy eigenstate of H: $H(t)|\text{dimer}\rangle = 0$.

- **Reference:** Phys. Rev. B 108, 155102 (2023).
- **Analysis:**
  - Verified the bipartite entanglement entropy against the analytic prediction from the paper.
    For $L = 14, 16, 18$:

    $$S_A \approx 1.386 \approx 2\ln 2 \tag{11}$$

    Because S_A evaluates to $\approx 2\ln 2$ for increasing L, the dimer scar satisfy the *Area Law* for entanglement: in one dimension, the entanglement entropy remains constant with increasing system size.
  - Computed the ranks of all 2-site, 3-site, and 4-site adjacent reduced density matrices:

Dimer scar	**RDM Rank**		
	2-sites	**3-sites**	**4-sites**
$\|\text{dimer}\rangle$	4	4	5

Table 1: RDM ranks for 2, 3, and 4 adjacent sites in the dimer scar state for $L = 18$.

2. Domain-Wall Conserving Spin-1/2 Model

- **Model:** Spin-1/2 model with domain-wall conserving dynamics.

  For a system L spins-$\frac{1}{2}$ on a chain, the Hamiltonian reads

$$H = \sum_{i=1}^{L} \left[\lambda \left(\sigma_i^x - \sigma_{i-1}^z \sigma_i^x \sigma_{i+1}^z\right) + \mu\, \sigma_i^z + J\, \sigma_i^z \sigma_{i+1}^z\right] \equiv H_\lambda + H_z + H_{zz}, \tag{12}$$

  where $\sigma_i^{x,y,z}$ are Pauli matrices defined on site i.

- **Reference:** Phys. Rev. B 101, 024306 (2020).

- **Analysis:**

  – Restricted study to analytically known scarred eigenstates.
  There are two towers of scars, both of length $L/2$ for OBC and $L/2+1$ for PBC.
  The first tower is described by:

$$|S_n\rangle = \frac{1}{n!\sqrt{\mathcal{N}(L,n)}} \left(Q^\dagger\right)^n |\Omega\rangle, \quad n = 0, \ldots, L/2-1\,(L/2) \tag{13}$$

  where $|\Omega\rangle = |0\cdots 0\rangle$ and

$$\mathcal{N}(L,n) = \begin{cases} \binom{L-n-1}{n} & \text{OBC} \\ \frac{L}{n}\binom{L-n-1}{n-1} & \text{PBC} \end{cases} \tag{14}$$

  (PBC not defined for $n = 0$, even though it describes the first scar of the tower, i.e. state $|\Omega\rangle$).
  $Q^\dagger$ is the ladder operator, defined as:

$$Q^\dagger = \sum_{i=1}^{L} (-1)^i P_{i-1}^0\, \sigma_i^+\, P_{i+1}^0, \tag{15}$$

  where $\sigma_j^\pm = \frac{1}{2}(\sigma_j^x \pm i\sigma_j^y)$ and $P_i^0 = \frac{1}{2}(1-\sigma_i^z)$ is the local projector onto spin down.
  The second tower, related to the first one, is described as

$$|S'_n\rangle = G|S_n\rangle = \frac{1}{n!\sqrt{\mathcal{N}(L,n)}} \left(Q'^\dagger\right)^n |\Omega'\rangle, \quad n = 0, \ldots, L/2-1\,(L/2) \tag{16}$$

  where $G = \prod_{i=1}^{L} \sigma_i^x$ is a $\mathbb{Z}_2$ transformation that flips all spins, $|\Omega'\rangle = |1\cdots 1\rangle$, and

$$Q'^\dagger = GQ^\dagger G = \sum_{i=1}^{L} (-1)^i P_{i-1}^1\, \sigma_i^-\, P_{i+1}^1, \tag{17}$$

  with $P_i^1 = \frac{1}{2}(1+\sigma_i^z)$ the local projector onto spin up.
  Both scar towers are annihilated by H_λ, which breaks U(1): $H_\lambda|S_n\rangle = H_\lambda|S'_n\rangle = 0$.

– Bipartite entanglement entropy computed and compared with theoretical values. For the states $|S_n\rangle$, we have an exact formula for the bipartite entanglement entropy. Following the original reference, this is given by:

$$S_A^{|S_n\rangle} = -\sum_{k=0}^{K}\sum_{s=\pm}\lambda_{k,s}\ln\lambda_{k,s}, \tag{18}$$

where $K = \min(n, \lfloor L_A/2 \rfloor)$ and $\lambda_{k,s}$ are the eigenvalues of the RDM ρ_A over subsystem A, which are

$$\lambda_{k,\pm}(L, L_A, n) = \frac{D_{1,k}m_{1,k} + D_{2,k}m_{2,k} \pm \sqrt{(D_{1,k}m_{1,k} - D_{2,k}m_{2,k})^2 + 4D_{1,k}D_{2,k}m_{2,k}^2}}{2\mathcal{N}} \tag{19}$$

where

$$\mathcal{N} = \mathcal{N}(L, n) \tag{20}$$
$$D_{1,k} = D_{1,k}(L_A) = \mathcal{N}(L_A, k) \tag{21}$$
$$D_{2,k} = D_{2,k}(L_A) = \mathcal{N}(L_A - 1, k - 1) \tag{22}$$
$$m_{1,k} = m_{1,k}(L - L_A) = \mathcal{N}(L - L_A, n - k) + \mathcal{N}(L - L_A - 1, n - k - 1) \tag{23}$$
$$m_{2,k} = m_{2,k}(L - L_A) = \mathcal{N}(L - L_A, n - k) \tag{24}$$
$$\tag{25}$$

For bipartite entanglement, $L_A = \frac{L}{2}$.
By taking the asymptotic limit $L \to \infty$ of Eq. (19) one can show that the bipartite ee scales logarithmically with system size. The bipartite entanglement entropy was numerically computed and its consistency with Eq. (19) was verified, where we chose $|S_4\rangle$ for L=18 sites (with OBC!):

$$S_A^{|S_4\rangle} = -\sum_{k=0}^{4}\sum_{s=\pm}\lambda_{k,s}\ln\lambda_{k,s} \tag{26}$$

which gives $S_A^{|S_4\rangle} \approx 1.22$, and it agrees with the numerical result.

– Ranks of adjacent 2-site, 3-site, and 4-site (adjacent) RDMs assessed, for both towers

$\|S_n\rangle$	**RDM Rank**		
	2-sites	**3-sites**	**4-sites**
n = 1	2	2	2
n = 2	3	5	5
n = 3	3	5	7
n = 4	3	5	7
n = 5	3	5	7
n = 6	3	5	7
n = 7	3	5	7
n = 8	3	5	6

Table 2: RDM ranks for 2, 3, and 4 adjacent sites in the $|S_n\rangle$ scar tower for $L = 18$.

$\|S'_n\rangle$	**RDM Rank**		
	2-sites	**3-sites**	**4-sites**
n = 1	2	2	2
n = 2	3	5	5
n = 3	3	5	7
n = 4	3	5	7
n = 5	3	5	7
n = 6	3	5	7
n = 7	3	5	5
n = 8	3	5	6

Table 3: RDM ranks for 2, 3, and 4 adjacent sites in the $|S'_n\rangle$ scar tower for $L = 18$.

The chain length L dependence of the 2,3,4-sites RDM of the scar at the top of both tower was investigated too.

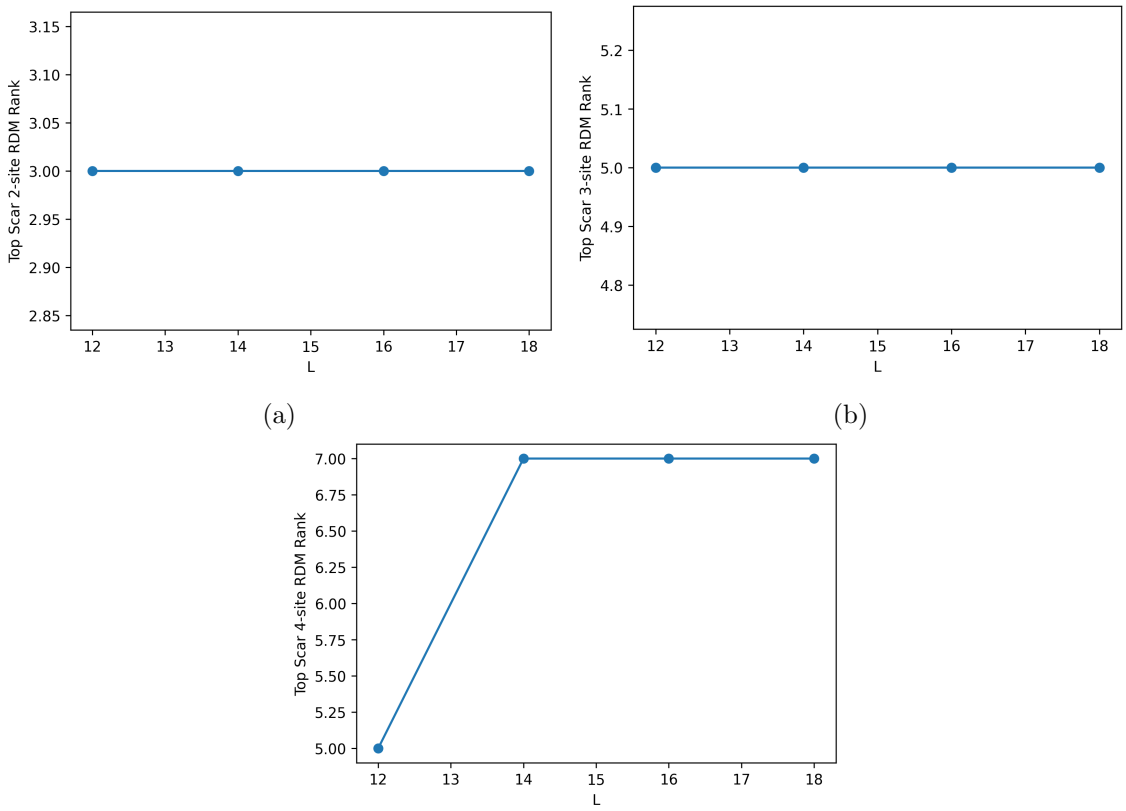

Figure 1: Innermost 2,3,4-sites RDM rank (Fig. (a), (b), (c) respectively) of the top scar of the tower $|S_n\rangle$ as a function of increasing L.

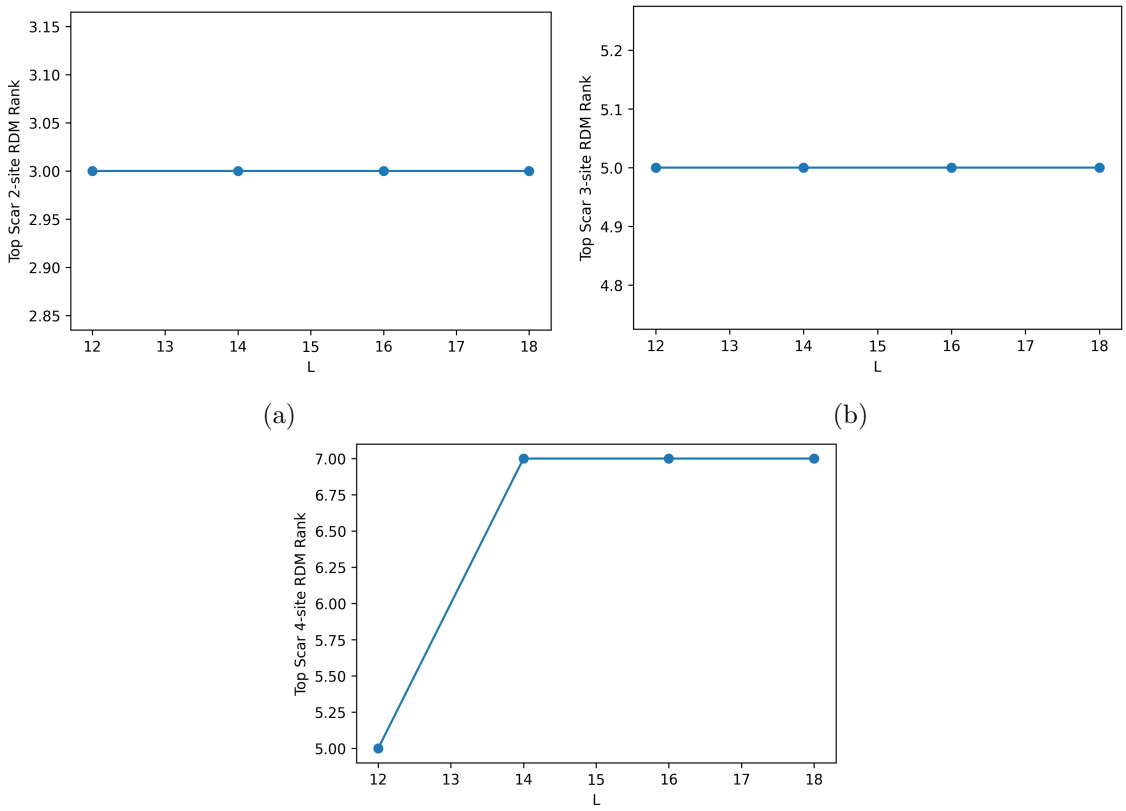

Figure 2: Innermost 2,3,4-sites RDM rank (Fig. (a), (b), (c) respectively) of the top scar of the tower $|S'_n\rangle$ as a function of increasing L.

3. Spin-1 XY Magnet Tower of Scars

- **Model:** Spin-1 XY model exhibiting a tower of scarred eigenstates.
  The Hamiltonian of the spin-1 XY model is:

$$H = J \sum_{\langle i,j \rangle} \left(S_i^x S_j^x + S_i^y S_j^y \right) + h \sum_i S_i^z + D \sum_i (S_i^z)^2 \,, \tag{27}$$

  where S_i^α $(\alpha = x, y, z)$ are spin-1 operators defined on the sites of a 1-dimensional chain of length L, and $\langle i, j \rangle$ denotes nearest neighbors.

- **Reference:** Phys. Rev. Lett. 123, 147201 (2019).

- **Analysis:**

  – Focused on exact scarred states with known analytic forms.
  There are two towers of scars, both of length $L + 1$.
  The first tower is described by:

$$|S_n\rangle = \mathcal{N}(L, n) \left(J^\dagger \right)^n |\Omega\rangle, \quad n = 0, \ldots, L \tag{28}$$

where $|\Omega\rangle = \bigotimes_i |m_i = -1\rangle$ and $\mathcal{N}(L,n) = \sqrt{(L-n)!/n!L!}$. $J^\dagger$ is the ladder operator, defined as:

$$J^\dagger = \frac{1}{2}\sum_{i=1}^{L}(-1)^i \left(S_i^+\right)^2, \tag{29}$$

where $S_i^\pm = S_i^x \pm iS_i^y$.
The second tower is given by

$$|S_n'\rangle \propto \sum_{i_1\neq\ldots\neq i_n} (-1)^{i_1+\ldots+i_n}\left(S_{i_1}^+ S_{i_1+1}^+\right)\ldots\left(S_{i_n}^+ S_{i_n+1}^+\right)|\Omega\rangle, \quad n=0,\ldots,L \tag{30}$$

Both scar towers are annihilated by the first term of (27), which breaks what is known as Q-SU(2) symmetry (a special SU(2) symmetry that only scars have - see the reference https://arxiv.org/pdf/2007.16207 for explanation): $J\sum_{\langle i,j\rangle}\left(S_i^x S_j^x + S_i^y S_j^y\right)|S_n\rangle = J\sum_{\langle i,j\rangle}\left(S_i^x S_j^x + S_i^y S_j^y\right)|S_n'\rangle = 0$.

– Bipartite entanglement entropy computed and compared with theoretical values. For the states $|S_n\rangle$, we have an exact formula for the bipartite entanglement entropy. Following the original reference, we can start from the reduced density matrix of a subsystem A:

$$\rho_A = \sum_{k=0}^{K}\lambda_k|k\rangle\langle k| \Rightarrow S_A^{|S_n\rangle} = -\sum_{k=0}^{K}\lambda_k \ln\lambda_k, \tag{31}$$

where $K = \min(n, L_A)$ and

$$\lambda_k = \frac{\begin{pmatrix} L-L_A \\ n-k \end{pmatrix}\begin{pmatrix} L_A \\ k \end{pmatrix}}{\begin{pmatrix} L \\ n \end{pmatrix}} \tag{32}$$

$|k\rangle$ are the associated eigenvectors. For bipartite entanglement, $L_A = \frac{L}{2}$.
By taking the asymptotic limit $L\to\infty$ of Eq. (31) one can show that the bipartite ee scales logarithmically with system size:

$$S_A^{|S_n\rangle} = \frac{1}{2}\left\{1 + \ln\left[\pi\nu\left(1-\nu\right)L\right]\right\} \tag{33}$$

where $\nu = \frac{n}{L}$. This formula is consistent with sub-volume law behavior, typical of many-body scars.
The bipartite entanglement entropy was numerically computed and its consistency with Eq. (31) was verified, where we chose $|S_5\rangle$ for L=10 sites (with OBC!):

$$S_A^{|S_5\rangle} = -\sum_{k=0}^{5}\lambda_k\ln\lambda_k, \quad \lambda_k = \frac{\binom{5}{5-k}\binom{5}{k}}{\binom{10}{5}} = \frac{\binom{5}{5-k}\binom{5}{k}}{252} \tag{34}$$

which gives $S_A^{|S_5\rangle} \approx 1.23$, and it agrees with the numerical result.

For generic L, $S_A^{|S_5\rangle}$ scales logarithmically with system size, i.e. $S_A^{|S_5\rangle} = \frac{1}{2}\ln\left(\frac{e\pi L}{8}\right)$. Because $S_A^{|S_5\rangle}$ is at the top of the tower - it has maximum possible value of entanglement entropy among the scars - we can assume that all scars have sub-volume scaling with system size, i.e. constant or at most logarithmic.

– Evaluated ranks of 2- to 4-site adjacent RDMs.

$\|S_n\rangle$	**RDM Rank**		
	2-sites	**3-sites**	**4-sites**
n = 0	1	1	1
n = 1	2	2	2
n = 2	3	3	3
n = 3	3	4	4
n = 4	3	4	5
n = 5	3	4	5
n = 6	3	4	5
n = 7	3	4	4
n = 8	3	3	3
n = 9	2	2	2
n = 10	1	1	1

Table 4: RDM ranks for 2, 3, and 4 adjacent sites in the $|S_n\rangle$ scar tower for $L = 10$.

$\|S'_n\rangle$	**RDM Rank**		
	2-sites	**3-sites**	**4-sites**
n = 0	1	1	1
n = 1	4	4	4
n = 2	6	8	8
n = 3	7	11	12
n = 4	7	12	15
n = 5	7	12	16
n = 6	7	12	15
n = 7	7	11	12
n = 8	6	8	8
n = 9	4	4	4
n = 10	1	1	1

Table 5: RDM ranks for 2, 3, and 4 adjacent sites in the $|S'_n\rangle$ scar tower for $L = 10$.
The scars $|S'_n\rangle$ are less rank-deficient than the $|S_n\rangle$ scars.

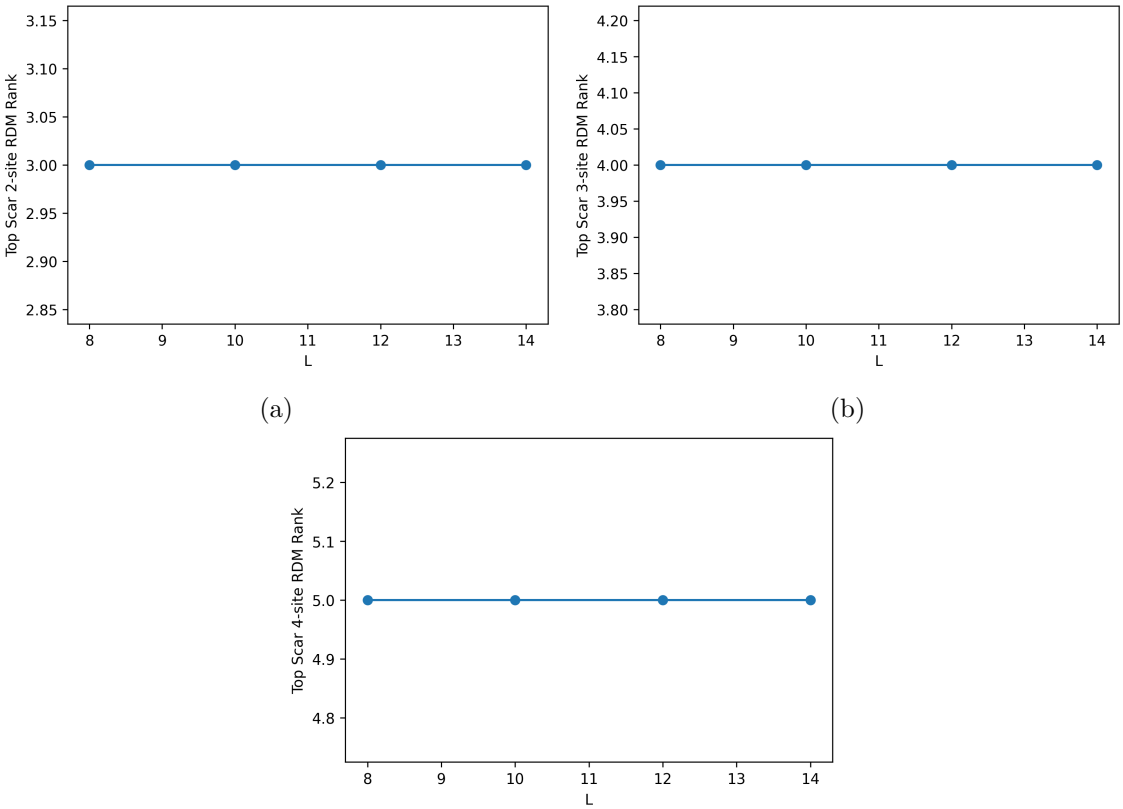

Figure 3: Innermost 2,3,4-sites RDM rank (Fig. (a), (b), (c) respectively) of the top scar of the tower $|S_n\rangle$ as a function of increasing L.

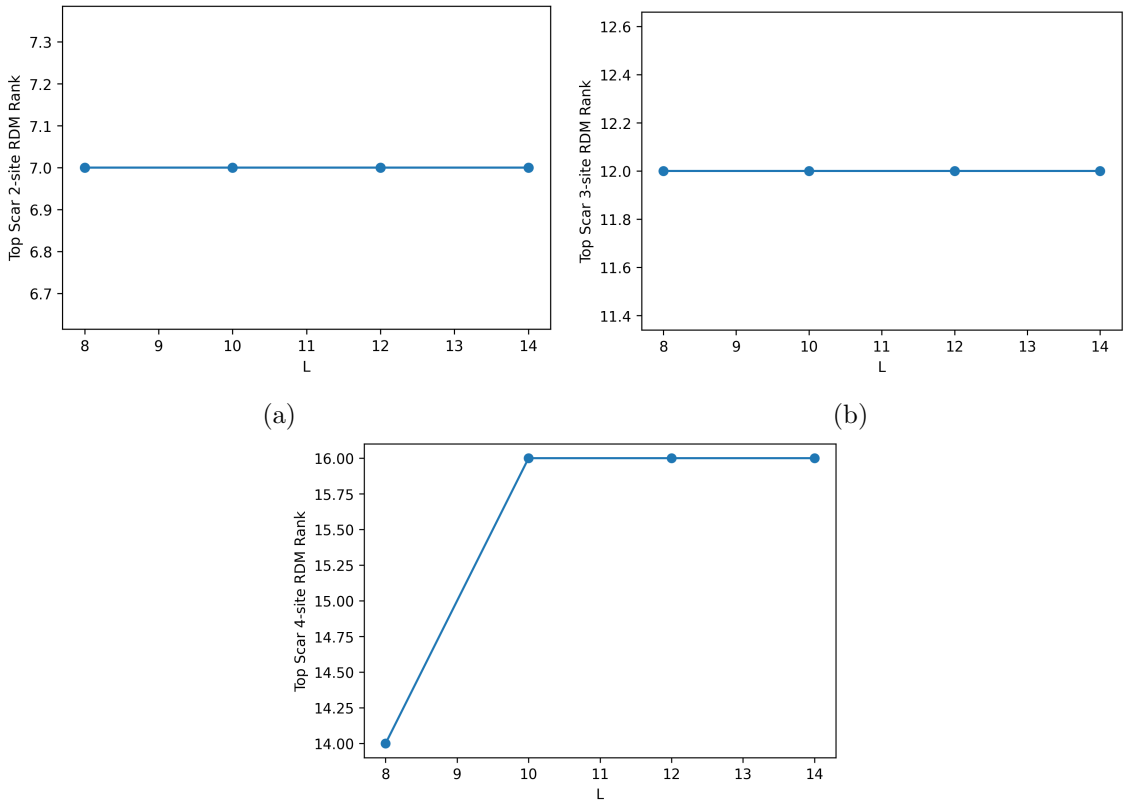

Figure 4: Innermost 2,3,4-sites RDM rank (Fig. (a), (b), (c) respectively) of the top scar of the tower $|S'_n\rangle$ as a function of increasing L.

4. Hubbard/Hirsch η-pairing Tower of Scars

- **Model:** 1D fermionic lattice model with on-site interactions and bond-charge coupling, known as the Hirsch model. The Hamiltonian is written as:

$$H = H_{\text{Hubbard}} + H_{\text{Hirsch}}, \tag{35}$$

where

$$H_{\text{Hubbard}} = -t \sum_{\langle i,j\rangle,\sigma} \left(c^\dagger_{i\sigma} c_{j\sigma} + \text{h.c.} \right) + U \sum_i n_{i\uparrow} n_{i\downarrow} - \mu \sum_{i,\sigma} n_{i\sigma}, \tag{36}$$

$$H_{\text{Hirsch}} = X \sum_{\langle i,j\rangle,\sigma} \left(n_{i\bar{\sigma}} + n_{j\bar{\sigma}} \right) \left(c^\dagger_{i\sigma} c_{j\sigma} + \text{h.c.} \right), \tag{37}$$

and $X \in \mathbb{R}$ is the Hirsch parameter that controls the strength of the bond-charge interaction. Here, $c^\dagger_{i\sigma}$ creates a fermion of spin $\sigma \in \{\uparrow, \downarrow\}$ at site i, and $n_{i\sigma} = c^\dagger_{i\sigma} c_{i\sigma}$. The sum $\langle i, j\rangle$ runs over nearest neighbors, and $\bar{\sigma}$ denotes the opposite spin of σ. Without loss of generality, we can set $\mu = 0$.

- **Reference:** Phys. Rev. B 102, 075132 (2020).
- **Analysis:**

  - There exists *three* towers of scarred states, all of length $L+1$ (L is the chain length). The first one is the known tower of η-pairing states, of the form:

$$|\eta_n\rangle = (\eta^\dagger)^n|0\rangle, \quad n = 0, \ldots, L \tag{38}$$

    where

$$\eta^\dagger = \sum_i (-1)^i c^\dagger_{i\uparrow} c^\dagger_{i\downarrow} \tag{39}$$

    is the η-pairing operator and $|0\rangle$ is the vacuum state. These states are exact eigenstates of H with energy $E_n = n\,U$, and they form a highest-weight tower under the SU(2) η-pairing symmetry. The scars are annihilated by the SU(2) η-pairing symmetry-breaking term H_{Hirsch}: $H_{\text{Hirsch}}|S_n\rangle = 0$.

    The other two towers can be obtained by applying an appropriate ladder operator on the η-pairing states. We call these towers τ-pairing states $|\tau_{m,n}\rangle$, and ς-pairing states $|\varsigma_n\rangle$:

$$|\tau_{m,n}\rangle = (\tau^\dagger)^m|\eta_n\rangle = (\tau^\dagger)^m(\eta^\dagger)^n|0\rangle \quad m = 0, \ldots, L \tag{40}$$

$$|\varsigma_n\rangle = \varsigma^\dagger|\eta_n\rangle = \varsigma^\dagger(\eta^\dagger)^n|0\rangle \tag{41}$$

    where

$$\tau^\dagger = \sum_i (-1)^i c^\dagger_{i\uparrow} c^\dagger_{i+1\uparrow} \tag{42}$$

$$\varsigma^\dagger = \sum_i (-1)^i \left(c^\dagger_{i\uparrow} c^\dagger_{i+1\downarrow} - c^\dagger_{i\downarrow} c^\dagger_{i+1\uparrow} \right) \tag{43}$$

    $\tau^\dagger$ creates a nearest-neighbor triplet $|\uparrow,\uparrow\rangle$ with momentum π, while $\varsigma^\dagger$ creates a nearest-neighbor singlet $|\uparrow,\downarrow\rangle - |\downarrow,\uparrow\rangle$ with momentum π. For PBC, we set $c^\dagger_{L+1\sigma} \equiv c^\dagger_{1\sigma}$. These states are again exact eigenstates of H with energy $E_n = n\,U$. Additionally, $|\tau_{m,n}\rangle$ has total spin $S = m$.
    Note that both $|\tau_{m,n}\rangle$, $|\varsigma_n\rangle$, unlike the η-pairing states, are in general not normalized, and therefore need to be normalized before looking at properties such as entanglement entropy or RDM rank.
    Both towers $|\tau_{m,n}\rangle$ and $|\varsigma_n\rangle$ are annihilated by the following three kinetic terms, which preserve spin and particle number while commuting with the η-pairing operator:

$$H_{\text{kin},1} = \sum_{j,\sigma} |h,\sigma\rangle\langle\sigma,h|_{j,j+1} + h.c. \tag{44}$$

$$H_{\text{kin},2} = \sum_j \left(|h,d\rangle + |d,h\rangle\right)\left(|\uparrow,\downarrow\rangle - |\downarrow,\uparrow\rangle\right)_{j,j+1} + h.c. \tag{45}$$

$$H_{\text{kin},3} = \sum_{j,\sigma} |d,\sigma\rangle\langle\sigma,d|_{j,j+1} + h.c. \tag{46}$$

where, following the notation of the original paper, we have defined the states on site j:

$$|h\rangle_j = |n_{j,\uparrow} = 0, n_{j,\downarrow} = 0\rangle \tag{47}$$
$$|d\rangle_j = |n_{j,\uparrow} = 1, n_{j,\downarrow} = 1\rangle \tag{48}$$
$$|\uparrow\rangle_j = |n_{j,\uparrow} = 1, n_{j,\downarrow} = 0\rangle \tag{49}$$
$$|\downarrow\rangle_j = |n_{j,\uparrow} = 0, n_{j,\downarrow} = 1\rangle \tag{50}$$

The original Hamiltonian (36) can be expressed in terms of these kinetic terms:

$$H_{\text{Hubbard}} = -t\left(H_{\text{kin},1} + H_{\text{kin},2} - H_{\text{kin},3}\right) + U\sum_j |d\rangle\langle d|_j, \tag{51}$$

$$H_{\text{Hirsch}} = X\left(H_{\text{kin},2} - 2H_{\text{kin},3}\right). \tag{52}$$

To show that the towers $|\tau_{m,n}\rangle$ and $|\varsigma_n\rangle$ are annihilated by the three kinetic terms

$$H_{\text{kin},a}|\tau_{m,n}\rangle = H_{\text{kin},a}|\varsigma_n\rangle = 0, \quad \text{for } a = 1,2,3. \tag{53}$$

one can first demonstrates that $|\tau_{m,0}\rangle$ and $|\varsigma_0\rangle$ are annihilated by them, then that

$$[H_{\text{kin},a}, \eta^\dagger]|\tau_{m,n}\rangle = [H_{\text{kin},a}, \eta^\dagger]|\varsigma_n\rangle = 0, \quad \text{for } a = 1,2,3. \tag{54}$$

– For the η-pairing states, we have an exact formula for the bipartite entanglement entropy. Following the original reference, we can start from the reduced density matrix of a subsystem A:

$$\rho_A = \sum_{k=0}^{K} \lambda_k |k\rangle\langle k| \Rightarrow S_A^{|\eta_n\rangle} = -\sum_{k=0}^{K} \lambda_k \ln \lambda_k, \tag{55}$$

where $K = \min(n, L_A)$ and

$$\lambda_k = \frac{\begin{pmatrix} L - L_A \\ n - k \end{pmatrix}\begin{pmatrix} L_A \\ k \end{pmatrix}}{\begin{pmatrix} L \\ n \end{pmatrix}} \tag{56}$$

$$|k\rangle = \sqrt{\frac{(L_A - k)!}{L_A! k!}}\left(\sum_{i=1}^{L_A} (-1)^i c_{i\uparrow}^\dagger c_{i\downarrow}^\dagger\right)^k |0\rangle_A \tag{57}$$

For bipartite entanglement, $L_A = \frac{L}{2}$.
By taking the asymptotic limit $L \to \infty$ of Eq. (55) one can show that the bipartite ee scales logarithmically with system size:

$$S_A^{|\eta_n\rangle} = \frac{1}{2}\left\{1 + \ln\left[\pi n\left(1 - \frac{n}{L}\right)\right]\right\} \tag{58}$$

consistent with sub-volume law behavior, typical of many-body scars.
The bipartite entanglement entropy was computed and its consistency with Eq. (55) was verified, where we chose $|\eta_6\rangle$ for L=12 sites:

$$S_A^{|\eta_6\rangle} = -\sum_{k=0}^{6} \lambda_k \ln \lambda_k, \quad \lambda_k = \frac{\binom{6}{6-k}\binom{6}{k}}{\binom{12}{6}} = \frac{\binom{6}{6-k}\binom{6}{k}}{924} \tag{59}$$

which gives $S_A^{|\eta_6\rangle} \approx 1.32$, and it agrees with the numerical result. The agreement was also verified for each one of the eigenvalues λ_k.

– Evaluated ranks of 2- to 4-site adjacent RDMs.
Note that, only for the tower $|\eta_n\rangle$, we can theoretically check the rank values from Eq. (55),(56): given that the RDM ρ_A is in its Schmidt form, its rank is simply the number of non-zero eigenvalues λ_k. All of these theoretical ranks do in fact match their numerical counterparts.

$\|\eta_n\rangle$	**RDM Rank**		
	2-sites	**3-sites**	**4-sites**
n = 0	1	1	1
n = 1	2	2	2
n = 2	3	3	3
n = 3	3	4	4
n = 4	3	4	5
n = 5	3	4	5
n = 6	3	4	5
n = 7	3	4	5
n = 8	3	4	5
n = 9	3	4	4
n = 10	3	3	3
n = 11	2	2	2
n = 12	1	1	1

Table 6: RDM ranks for 2, 3, and 4 adjacent sites in the $|\eta_n\rangle$ scar tower for $L = 12$.

RDM Rank ($m = 1$)			
n	2-sites	3-sites	4-sites
0	4	4	4
1	7	8	8
2	8	11	12
3	8	12	15
4	8	12	16
5	8	12	16
6	8	12	16
7	8	12	15
8	8	11	12
9	7	8	8
10	4	4	4
11	-	-	-
12	-	-	-

RDM Rank ($m = 2$)			
n	2-sites	3-sites	4-sites
0	4	6	8
1	7	11	15
2	8	14	20
3	8	15	23
4	8	15	24
5	8	15	23
6	8	14	20
7	7	11	15
8	4	6	8
9	-	-	-
10	-	-	-
11	-	-	-
12	-	-	-

RDM Rank ($m = 3$)			
n	2-sites	3-sites	4-sites
0	4	6	8
1	7	11	15
2	8	14	20
3	8	15	22
4	8	14	20
5	7	11	15
6	4	6	8
7	-	-	-
8	-	-	-
9	-	-	-
10	-	-	-
11	-	-	-
12	-	-	-

RDM Rank ($m = 4$)			
n	2-sites	3-sites	4-sites
0	4	6	8
1	7	11	14
2	8	13	16
3	7	11	14
4	4	6	8
5	-	-	-
6	-	-	-
7	-	-	-
8	-	-	-
9	-	-	-
10	-	-	-
11	-	-	-
12	-	-	-

RDM Rank ($m = 5$)			
n	2-sites	3-sites	4-sites
0	4	4	4
1	6	6	6
2	4	4	4
3	-	-	-
4	-	-	-
5	-	-	-
6	-	-	-
7	-	-	-
8	-	-	-
9	-	-	-
10	-	-	-
11	-	-	-
12	-	-	-

RDM Rank ($m = 6$)			
n	2-sites	3-sites	4-sites
0	1	1	1
1	-	-	-
2	-	-	-
3	-	-	-
4	-	-	-
5	-	-	-
6	-	-	-
7	-	-	-
8	-	-	-
9	-	-	-
10	-	-	-
11	-	-	-
12	-	-	-

Table 7: RDM ranks for states $|\tau_{m,n}\rangle$ for various m and n, across 2-, 3-, and 4-sites RDMs for $L = 12$. The $-$ symbol indicates that the corresponding state is forbidden by the Pauli exclusion principle, and thus the density matrix is not defined in that case.

$\|\varsigma_n\rangle$	RDM Rank		
	2-sites	**3-sites**	**4-sites**
n = 0	6	6	6
n = 1	11	12	12
n = 2	12	17	18
n = 3	12	18	23
n = 4	12	18	24
n = 5	12	18	24
n = 6	12	18	24
n = 7	12	18	23
n = 8	12	17	18
n = 9	11	12	12
n = 10	6	6	6
n = 11	-	-	-
n = 12	-	-	-

Table 8: RDM ranks for 2, 3, and 4 adjacent sites in the $|\varsigma_n\rangle$ scar tower for $L = 12$.

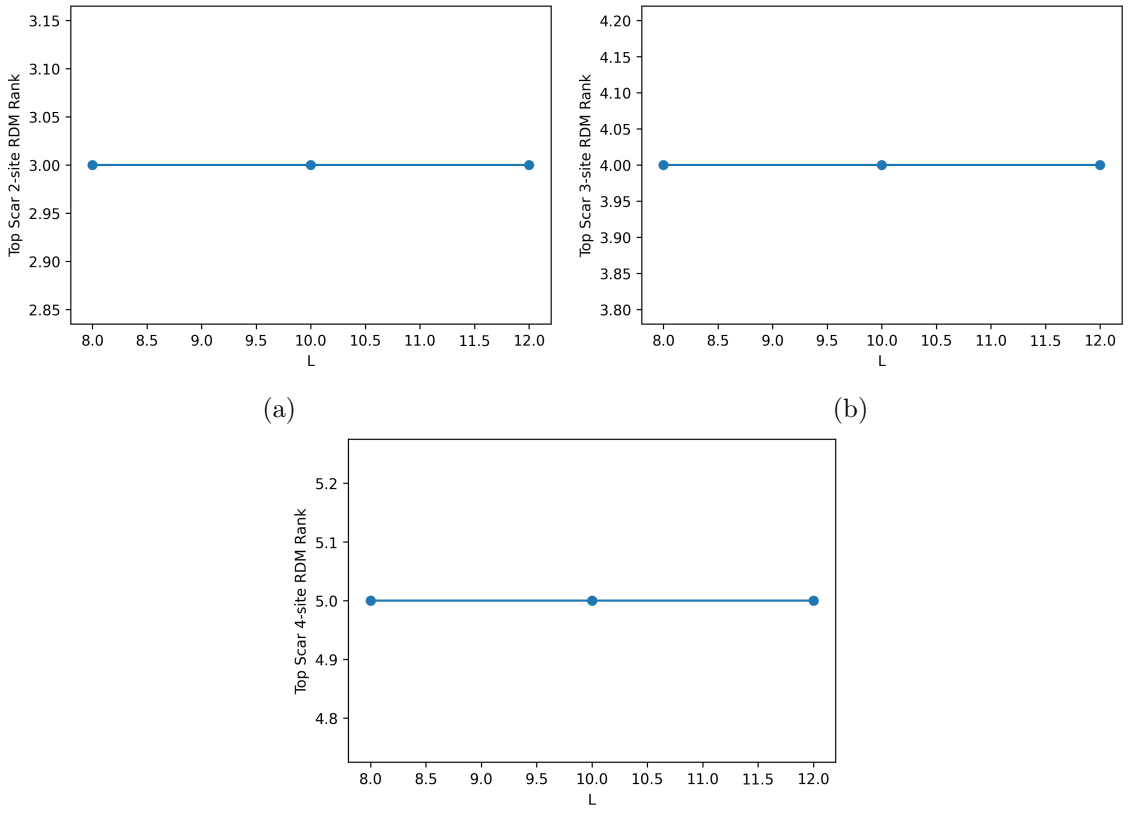

Figure 5: Innermost 2,3,4-sites RDM rank (Fig. (a), (b), (c) respectively) of the top scar ($n = L/2$) of the tower $|\eta_n\rangle$ as a function of increasing L.

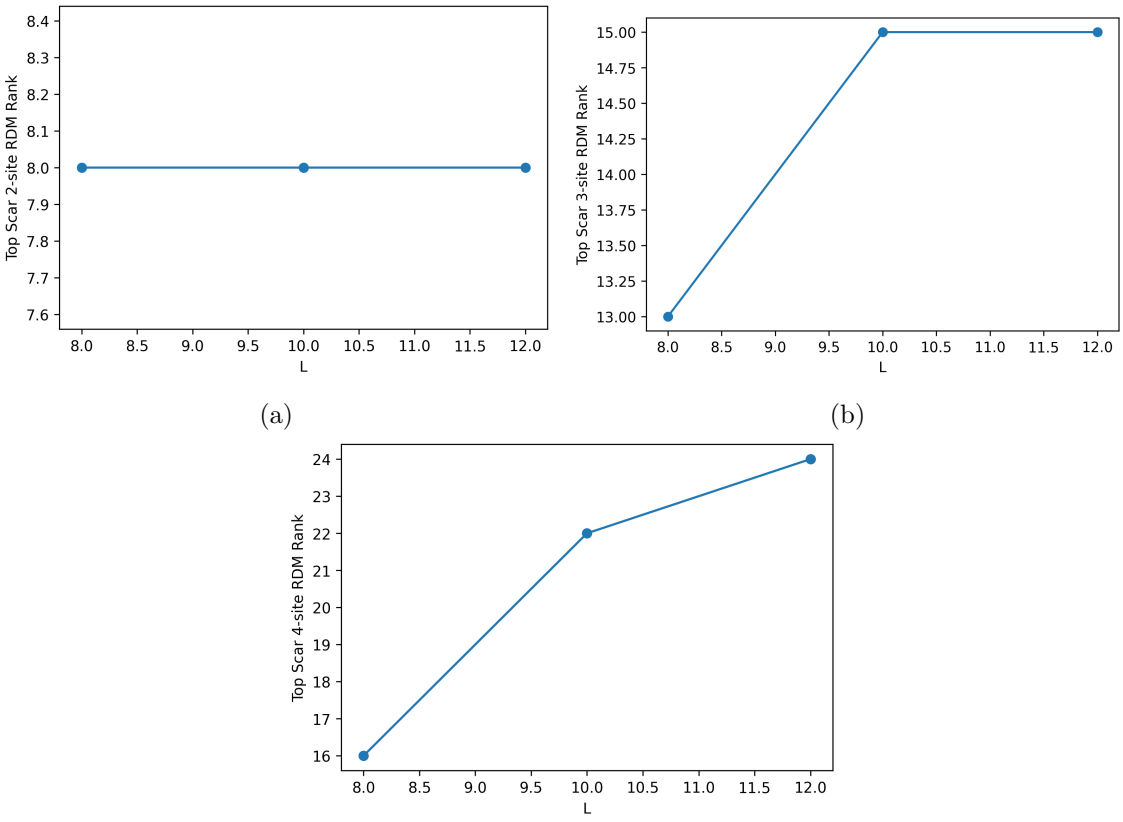

(a) (b)

(c)

Figure 6: Innermost 2,3,4-sites RDM rank (Fig. (a), (b), (c) respectively) of the top scar ($m = 2, n = 2, 3, 4$) of the tower $|\tau_{m,n}\rangle$ as a function of increasing L.

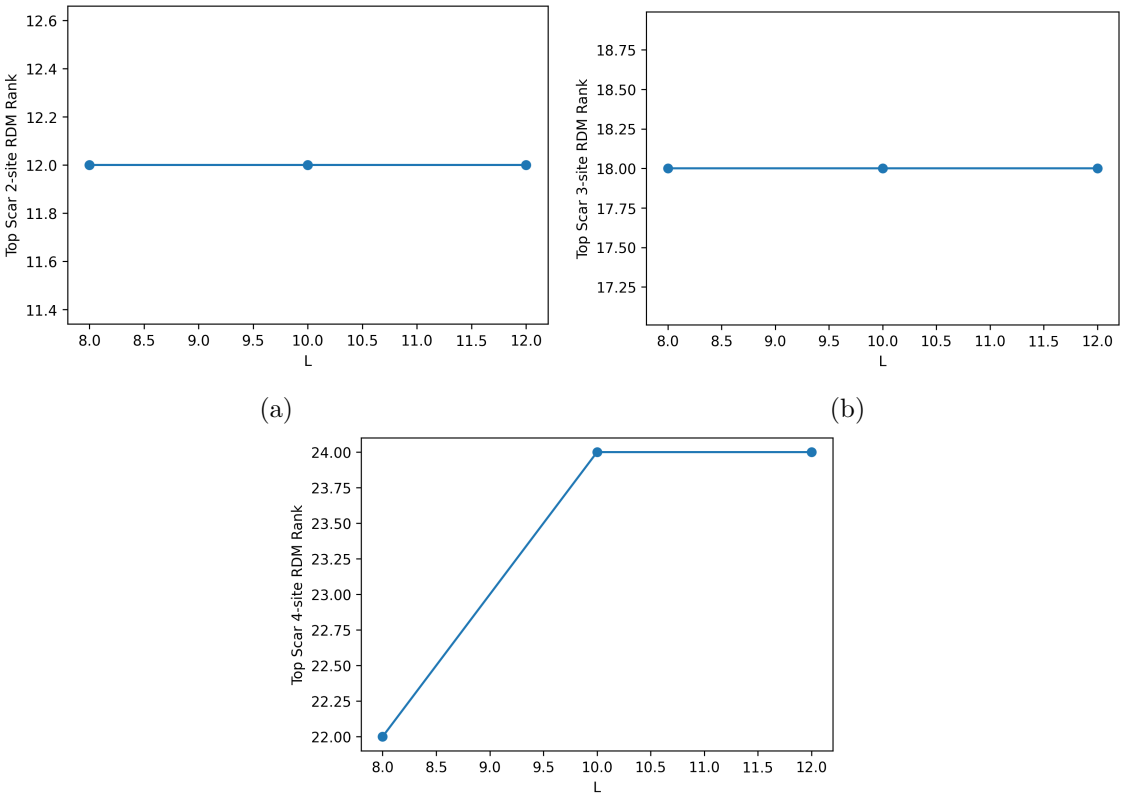

Figure 7: Innermost 2,3,4-sites RDM rank (Fig. (a), (b), (c) respectively) of the top scar ($n = L/2 - 1$) of the tower $|\varsigma_n\rangle$ as a function of increasing L.

Conclusion

Across all models, the focus was placed exclusively on scarred states with known exact analytic expressions. The investigations confirm key entanglement features and low-rank structure of adjacent reduced density matrices, serving as diagnostics of scarred nonthermal behavior without requiring access to the full spectrum.